Development 135, 1049-1058 (2008) doi:10.1242/dev.013359

R-spondin 2 is required for normal laryngeal-tracheal, lung and limb morphogenesis

Sheila M. Bell[1], Claire M. Schreiner[2], Susan E. Wert[1], Michael L. Mucenski[1], William J. Scott[2] and Jeffrey A. Whitsett[1,*]

Herein, we demonstrate that Lrp6-mediated R-spondin 2 signaling through the canonical Wnt pathway is required for normal morphogenesis of the respiratory tract and limbs. We show that the *footless* insertional mutation creates a severe hypomorphic R-spondin 2 allele (*Rspo2*^{Tg}). The predicted protein encoded by *Rspo2*^{Tg} neither bound the cell surface nor activated the canonical Wnt signaling reporter TOPFLASH. Rspo2 activation of TOPFLASH was dependent upon the second EGF-like repeat of Lrp6. *Rspo2*$^{Tg/Tg}$ mice had severe malformations of laryngeal-tracheal cartilages, limbs and palate, and lung hypoplasia consistent with sites of *Rspo2* expression. *Rspo2*$^{Tg/Tg}$ lung defects were associated with reduced branching, a reduction in TOPGAL reporter activity, and reduced expression of the downstream Wnt target *Irx3*. Interbreeding the *Rspo2*^{Tg} and *Lrp6*$^{-}$ alleles resulted in more severe defects consisting of marked lung hypoplasia and absence of tracheal-bronchial rings, laryngeal structures and all limb skeletal elements.

KEY WORDS: R-spondin 2, Lrp6, Lung, Larynx, Trachea, Limb, Development, Wnt signaling, Sp8, Mouse

INTRODUCTION

The canonical Wnt signaling pathway is regulated by the binding of Wnt ligands with a complex of one of 10 frizzled (Fzd) transmembrane receptors and low density lipoprotein receptor related protein 5 or 6 (Lrp) resulting in stabilization of intracellular β-catenin (for a review, see Logan and Nusse, 2004). β-Catenin translocates to the nucleus and interacts with lymphoid enhancer factor (Lef)/T-cell factor (Tcf) transcription factors to alter gene transcription. Lrp6-mediated activation of the canonical Wnt signaling pathway also occurs in response to a new family of ligands: the R-spondins (Rspo) (Kazanskaya et al., 2004; Nam et al., 2006; Wei et al., 2007).

Disruption of the Wnt signaling pathway alters normal development of the lung and limb. Murine lung development begins at E9.5 as the foregut endoderm invaginates into the surrounding mesenchyme. Lung morphogenesis is dependent upon mesenchymal-epithelial interactions that promote branching of lung tubules. Primary branching forms the two bronchi, whereas asymmetric secondary branching, which occurs between E10 and E11.5, defines the number of airways and lobulation. Continued proximodistal branching generates the conducting airways that lead to the alveoli in the mature lung. High levels of Wnt signaling, indicated by the TOPGAL reporter, occur in the epithelium and mesenchyme adjacent to the proximal airways between E10.5 and E12.5 (De Langhe et al., 2005). The early epithelium expresses *Wnt7b* and *Lrp6*, whereas the mesenchyme expresses *Wnt2a* (De Langhe et al., 2005; Wang et al., 2005). Both tissues express *Wnt11*, *Wnt5a* and β-catenin (Li et al., 2002; Tebar et al., 2001; Weidenfeld et al., 2002). *Wnt5a*$^{-/-}$ fetuses exhibit truncation of the trachea, overexpansion of distal airways and disrupted lung maturation (Li et al., 2002). Lung hypoplasia and defects in pulmonary vessel smooth muscles were observed in *Wnt7b*$^{-/-}$ mice (Shu et al., 2002). Removal of β-catenin expression in the respiratory epithelium resulted in a failure of distal airway formation (Mucenski et al., 2003).

Canonical Wnt signaling is also required for normal limb formation. Cells within the emerging limb bud ventral ectoderm will form the apical ectodermal ridge (AER) (Bell et al., 2003b). The mature AER is localized at the limb bud apex and required for proximodistal elongation of the limb. The absence of *Wnt3* or β-catenin expression in murine AER precursor cells disrupts AER formation, resulting in distal limb truncations (Barrow et al., 2003). The AER also fails to form in embryos that lack *Lef* and *Tcf* (Galceran et al., 1999). *Lrp6* deletion causes limb abnormalities attributed to AER deficiencies (Pinson et al., 2000).

Reminiscent of *Lrp6*$^{-/-}$, the hindlimbs of fetuses homozygous for the *footless* mutation lack either the entire paw (autopod) or the posterior digits and, frequently, the fibula (Bell et al., 2003a). *footless* homozygotes also lack right forelimb digits 1 and/or 2. Distal telephalanges and fingernails were missing on formed digits. These malformations were previously correlated with regional deficiencies in AER formation at E10.5. Homozygous *footless* progeny had cleft palate and died of unknown causes at birth.

Herein, we tested the hypothesis that integration of the *footless* transgene affected a component of the Wnt signaling pathway critical for formation of limbs and the respiratory tract. Transgene integration disrupted the R-spondin 2 (*Rspo2*) gene, creating a mutant allele: *Rspo2*^{Tg}. We present data that *Rspo2*$^{Tg/Tg}$ fetuses possess laryngeal-tracheal cartilage malformations and lung hypoplasia. The limb and lung phenotypes were exacerbated by the absence of *Lrp6*.

MATERIALS AND METHODS

Mouse models and analysis

Animal protocols were approved by the Institutional Animal Care and Use Committee in accordance with NIH guidelines. Detection of a vaginal plug was defined as E0.5. *Lrp6*-deficient animals were provided by Dr W. Skarnes (Wellcome Trust Sanger Institute). TOPGAL mice were provided by Dr E. Fuchs (The Rockefeller University). For Cre activation, animals

[1]Section of Neonatology, Perinatal and Pulmonary Biology and [2]Division of Developmental Biology, Cincinnati Children's Hospital Medical Center and The University of Cincinnati College of Medicine, Cincinnati, OH 45229, USA.

*Author for correspondence (e-mail: jeff.whitsett@cchmc.org)

Accepted 2 January 2008

were fed food containing doxycycline as described (Mucenski et al.; 2003). E18.5 fetal crown-rump lengths, weights and body circumference under the forelimbs were recorded. Lung, trachea and laryngeal tissues were dissected and weighed prior to fixation. For visualization of cartilage and bone, alcohol (95%) fixed, skinned fetuses and trachea were stained with Alizarin Red and Alcian Blue, and cleared in graded 2% KOH:glycerol solutions (100:0-0:100). Paraformaldehyde (4%) fixed tissue was embedded in paraffin wax. Genomic DNA from the fetal viscera was used for genotyping.

Gene and cDNA characterization

RT-PCR and Northern blot analyses were performed on E11 embryo total RNA. RNA was reversed transcribed using Oligo dT and Superscript II (Invitrogen) and amplified with the Rspo2 primer pairs 5′-GCGGG-TGTCGGCAAACTTTTTC-3′ and 5′-ATCTGGGGCTCGGTGTCCAT-AATAC-3′ (818 bp product spanning exons 1-3); 5′-CATCAGGGTA-TTATGGACACCGAG-3′ and 5′-TGCTCTTGGGCTCTCTCAATCAGC-3′ (spanning exons 3-6); and 5′-GCGGGTGTCGGCAAACTTTTTC-3′ with the SV40 primer AGGTAGTTTGTCCAATTATG-3′ (spanning exon 1 into transgene). Products were subcloned and sequence verified. The 818 bp product was hybridized to northern blots.

Alkaline phosphatase-Rspo2 fusion constructs and cell lines

The Rspo2 cDNA was PCR amplified using a common *Nhe*I flanked 5′ primer 5′-TCCAGCTAGCTAGCCACCATGCGTTTTTGCCTC-3′ with either 5′-AGTAGATCTTGCACATCTGTTCATATCTGG-3′, 5′-CGGAA-GATCTACCTTCTACACATTCCAT-3′, 5′-TCCGGAAGATCTCTTTGG-TGTTCTCTTTCC-3′ or 5′-CCCGAGATCTTGGTTCACTCTGTC-3′. *Nhe*I/*Bgl*II digested PCR products were subcloned into APTAG5 (GenHunter). Sequence verified constructs were transfected into HEK293T cells and clonal cell lines established by Zeocin (Invitrogen) selection (600 μg/ml). Clones were maintained in 300 μg/ml Zeocin. For conditioned media, subconfluent cell cultures were incubated in serum containing growth media or OptiPro (Invitrogen) for 3-4 days. As a negative control, conditioned media was collected from APTAG4 cells (GenHunter) secreting AP.

Alkaline phosphatase activity assays

AP assay reagents A and S (GenHunter) were used according to the manufacturer instructions to quantitate AP activity in conditioned media, eluates, or cell lysates. For cell binding assays, subconfluent cultures of HEK293T, MLE15 or HeLa cells were rinsed in Hanks Balanced Salt Solution (HBSS), incubated with conditioned media containing equivalent AP activity units for 1.5 hours at room temperature, rinsed five times in HBSS and lysed in 0.5 ml of AP lysis buffer (GenHunter). In some experiments, heparin (Sigma) was added with the media. Lysates were heated at 65°C 15 minutes to inactivate endogenous AP activity. Average activity from triplicate wells is presented.

Heparin binding assay

Conditioned media were absorbed to 300 μl of heparin agarose (Sigma) at 4°C with rocking for 48 hours. The agarose was pelleted by centrifugation and washed by sequential resuspensions in 50 mM Tris (pH 8.0) with the indicated amount of NaCl. AP activity present in each eluate was determined.

Luciferase assays

HEK293T cells (~1.5×10^5/well) were co-transfected with TOPFLASH (Upstate), pRL-TK (Promega) and Lrp6 plasmids using Fugene 6 (Roche). Conditioned medium containing equivalent levels of AP activity was added 24 hours post-transfection and incubated 24 hours prior to cell lysis. Firefly luciferase and *Renilla* luciferase activity were determined using the Promega Dual Luciferase assay. Each assay was performed in triplicate and all experiments were performed at least twice.

β-Gal assays

E11.5 lung buds from 46-54 somite embryos were dissected and frozen at –70 until genotyped. Each lung was resuspended in 25 μl of lysis reagent. Two 5 μl aliquots were incubated with Galacton-Star substrate (Applied Biosystems) for 90 minutes and light emission read in a Monolight 3010 luminometer. The amount of protein present in each lysate was determined in duplicate using the Bio-Rad protein reagent according to the manufacturer's directions. For each lung, β-galactosidase activity was normalized to total protein.

For whole-mount visualization, lungs were fixed for 1 hour, rinsed three times in PBS, and developed for 5 hours in 5 mM $K_3Fe(CN)_6$, 5 mM $K_4Fe(CN)_6$, 2 mM $MgCl_2$, 0.01% sodium deoxycholate, 0.2% NP-40 and 1 mg/ml X-Gal.

Lung organ culture

Dissected E11.5 lung buds were placed onto Nucleopore Trach-etched 8 μm membranes (Whatman) in wells containing 0.5 ml of DMEM containing 10% FCS, 2 mM glutamine, 100 units/ml penicillin/streptomycin and 0.5 ml of the indicated conditioned medium. Explants were incubated at 37°C with 5% CO_2 and photographed every 24 hours.

Lrp6 constructs

Full length mouse Lrp6 with a single C-terminal Flag tag was provided by Dr R. Lang (CCHMC). To create ΔEGF2 Lrp6, the plasmid was partially digested with *Eco*RV and religated, deleting amino acids 359-641. To create ΔEGF3-4 Lrp6, the *Xba*I/*Xho*I 7552 bp vector-Lrp6 fragment was isolated. PCR introduced an *Xho*I site at amino acid 1247; a product spanning from 1247 to the end of the flag epitope was amplified. Ligation resulted in a construct deleting amino acids 638-1247.

Western blots

Samples were boiled in Laemmli buffer, electrophoresed under denaturing conditions and blotted onto nitrocellulose. Rspo2-conditioned media were concentrated using Centricon 30 centrifugal filter units (Millipore). Rspo2AP fusion proteins were detected using a rabbit polyclonal antibody to human placental AP (1:2000) (GenHunter). Lrp6 constructs were transfected into HEK293T cells and cell lysates generated 48 hours later in the presence of protease inhibitor cocktail (Sigma). The Lrp6-flag epitope was detected using monoclonal M2 anti-Flag antibody (Sigma) (1:10,000), an anti-rabbit IgG peroxidase conjugate (Calbiochem) (1:10,000) and ECL western blotting detection reagent (GE Healthcare).

Immunohistochemistry

Paraffin wax-embedded tissue was sectioned at 5 μm, dewaxed, rehydrated in graded ethanols, subjected to antigen retrieval, and endogenous peroxidase activity was quenched in methanol and H_2O_2 for 15 minutes. Antibodies requiring antigen retrieval were FoxJ1 (using 0.1 M citrate buffer, pH 6.0 and heat) and Pecam1 (15 minutes trypsin digestion at 37°C). Biotinylated secondary antibodies (1:200, Vector Laboratories) were detected using an avidin-biotin-horseradish-peroxidase detection system (ABC reagent, Vector Laboratories, Burlingame, CA). Sections were counterstained with Nuclear Fast Red. As a negative control, primary antibody was omitted on some slides. Primary antibodies used were rabbit anti-FoxJ1 (1:5000; from Dr Robert Costa), mouse anti-α-smooth muscle actin (1:10,000; monoclone 1a4, Sigma), rabbit anti-proSP-C and rabbit anti-CCSP (1:1000, Seven Hills Bioreagents), rat anti-Pecam-1 (1:500; monoclonal CD-31, Pharmigen), and hamster anti-T1-alpha (1:500; Clone 8.1, Iowa Developmental Studies Hybridoma Bank).

Real-time RT-PCR

cDNA was generated from ectodermal hulls of stage 1.5 and 4 hindlimb buds or E11.5 lung buds, and real time RT-PCR was performed using gene specific primers as previously described (Bell et al., 2005). At least two independent cDNA samples generated from pooled tissues were used. All values were normalized to α-tubulin within the sample.

RESULTS

Identification of the site of insertional mutagenesis

Previous studies determined that the *footless* transgene insertional mutation was attributable to a single integration site on mouse chromosome 15 (Bell et al., 2003a). Using genomic fragments immediately flanking the integration site, overlapping clones were isolated and characterized from a genomic 129S/SvJ library. NCBI

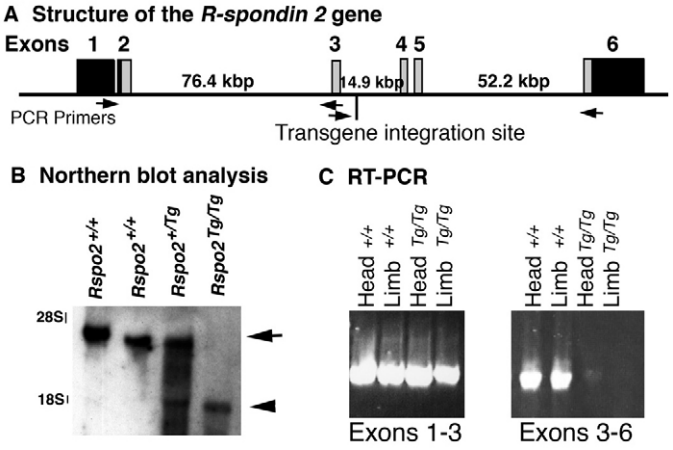

Fig. 1. *Rspo2* is disrupted in the transgene insertional mutation *footless*. (**A**) *Rspo2* gene. Untranslated exons are shown in black, arrows indicate the location of PCR primers. (**B**) Northern blot of E11.0 embryo total RNA. Arrow indicates full-length transcript; arrowhead indicates alternatively spliced transcript. (**C**) RT-PCR of E11.0 embryonic cDNA. The primers for exons 3-6 spanning the transgene integration site detected only small amounts of product in $Rspo2^{Tg/Tg}$ embryos.

Blast analysis of sequenced clones localized the transgene integration site to the third intron of the R-spondin 2 (*Rspo2*) gene (Kazanskaya et al., 2004; Lowther et al., 2005; Nam et al., 2006), denoted the $Rspo2^{Tg}$ allele. The entire *Rspo2* gene uses six exons and spans ~150 kb (Fig. 1A). No other transcripts have been mapped to this genomic region. EST analysis and whole-mount in situ hybridization assays confirmed that the full-length transcript contains an ~1.6 kb 5′ untranslated region and includes sequences present within NM_172815, EST BB707197 and EST AK011587.

Although transgene integration did not result in excision of any exons, we evaluated *Rspo2* expression by northern blot analysis, RT-PCR and whole-mount in situ hybridization assays. Northern blot analysis of total RNA detected an ~4.5 kb band in $Rspo2^{+/+}$ and $Rspo2^{+/Tg}$ samples. A smaller transcript was also present in $Rspo2^{+/Tg}$ and was the only band in $Rspo2^{Tg/Tg}$ RNA (Fig. 1B). Using exon specific primers, the alternate band was characterized by RT-PCR. A product spanning exons 1-3 was readily amplified from $Rspo2^{+/+}$ and $Rspo2^{Tg/Tg}$ cDNA. By contrast, an exon 3-6 PCR product was robustly amplified from $Rspo2^{+/+}$ cDNA, but only a negligible amount of product was generated from $Rspo2^{Tg/Tg}$ cDNA, indicating a very low level of full-length transcript production in $Rspo2^{Tg/Tg}$ embryos (Fig. 1C). Using exon 1 and SV40 primers, a PCR product was amplified from $Rspo2^{Tg/Tg}$ cDNA. Sequence analysis indicated that exon 3 splices in frame to a cryptic splice-acceptor in the transgene, resulting in the potential production of a Rspo2-CAT fusion protein containing amino acids 1-94 of Rspo2 and 148-219 of CAT (data not shown).

The exon 1-3 and 3-6 PCR products were used to generate antisense riboprobes for whole-mount in situ hybridization assays. At E10.5, *Rspo2* mRNA was detected in the AER of the limb buds from wild-type embryos using either riboprobe (Fig. 3B, data not shown). In $Rspo2^{Tg/Tg}$ embryos, the probe spanning exons 1-3 detected *Rspo2* expression within the AER and other locations, whereas the probe for exons 3-6 failed to detect mRNA expression anywhere in the embryo (data not shown). Integration of the transgene generated a severe hypomorphic allele of the mouse *Rspo2* gene that preferentially splices from exon 3 of *Rspo2* into the transgene.

Secretion of Rspo2 and activation of canonical Wnt signaling

The murine *R-spondin* gene family consists of four structurally similar members located on distinct chromosomes. Rspo2 is a 243 amino acid protein comprising a 21 amino acid signal peptide followed by a cysteine-rich region (amino acids 40-80 encoded by exon 3), a furin-like domain (amino acids 89-144 encoded by exon 4), a thrombospondin type 1 (TSP1) domain (amino acids 148-203 encoded by exon 5) and a C-terminal highly charged region (amino acids 207-243 encoded by exon 6) (Fig. 2A). Alkaline phosphatase (AP) was fused to the C-terminus of either full-length Rspo2 (Rspo2AP) or domain deletion mutants. To create the truncated protein encoded by $Rspo2^{Tg}$, amino acids 96-243 (Δ96-243AP) were deleted. Δ148-243AP removed the TSP1 and highly charged domains of Rspo2. Δ212-243AP removed the highly charged C-terminus. Stable HEK293T cell lines expressing each construct secreted AP into the media (data not shown). Western blot analysis confirmed the presence of correctly sized Rspo2-AP fusion proteins (Fig. 2B) demonstrating that all of the Rspo2-AP fusion proteins were secreted.

The TSP1 domain of Rspo2 is closely related to the single TSP1 domain in mindin and fifth TSP1 domain in F-spondin, both previously shown to directly interact with heparin (Feinstein et al., 1999; Tzarfaty-Majar et al., 2001). TSP1 domains identified in other heparin-binding signaling molecules, including HB-GAM and midkine, form a heparin binding β-sheet structure (Kilpelainen et al., 2000). The basic C-terminal domain of Rspo2 (Fig. 2A) is similar to that found in growth factors that interact with extracellular matrix proteins on cell surfaces (Houck et al., 1992; LaRochelle et al., 1991). The ability of Rspo2 to interact with the cell surface was evaluated by absorbing conditioned media containing Rspo2AP fusion proteins to HEK293T, HeLa and MLE15 cells. Both the full-length and Δ212-243AP fusion proteins bound the cell surface of all cell types with greatest binding detected with Rspo2AP (Fig. 2C, data not shown). No cell-surface binding was observed with media containing AP, Δ96-243AP or Δ148-243AP. Rspo2AP and Δ212-243AP cell-surface interactions were dose-dependently displaced with heparin (see Fig. S1 in the supplementary material). To confirm direct interactions between Rspo2 fusion proteins and heparin, conditioned media were absorbed to heparin-agarose. The absorbed agarose was sequentially washed with buffers containing increasing amounts of NaCl, and AP activity was evaluated in the eluates. AP, Rspo2 Δ96-243AP and Rspo2 Δ148-243AP were poorly retained by the heparin agarose. Consistent with the cell binding assays, Rspo 2AP exhibited a higher affinity for heparin agarose than did Rspo2 Δ212-243AP (Fig. 2D). These data indicate that Rspo2 interacts with cell surface heparin sulfate proteoglycans, that the TSP1 domain is critical for this interaction and that amino acids 212-243 of Rspo2 potentiate heparin binding. Homologous domains in mRspo3 are required for Rspo3 binding to heparin sepharose (Nam et al., 2006).

Rspo family members activate the canonical Wnt signaling pathway by interacting with Lrp6 (Kazanskaya et al., 2004; Nam et al., 2006; Wei et al., 2007). To evaluate the biological activity of the Rspo2-AP fusion proteins and to further define the domains required for interaction with Lrp6, HEK293T cells were transfected with the luciferase Wnt signaling reporter TOPFLASH and pRL-TK (Renilla luciferase under control of the HSV-Tk promoter), and exposed to the indicated conditioned media. TOPFLASH reporter activation was observed in the presence of Rspo2AP, Δ212-243AP and, to a lesser extent, Δ148-243AP, but was not induced by Δ96-243AP (Fig. 2E). Thus, the truncated Rspo2 product encoded by the $Rspo2^{Tg}$ allele would not be able to activate the canonical Wnt signaling pathway.

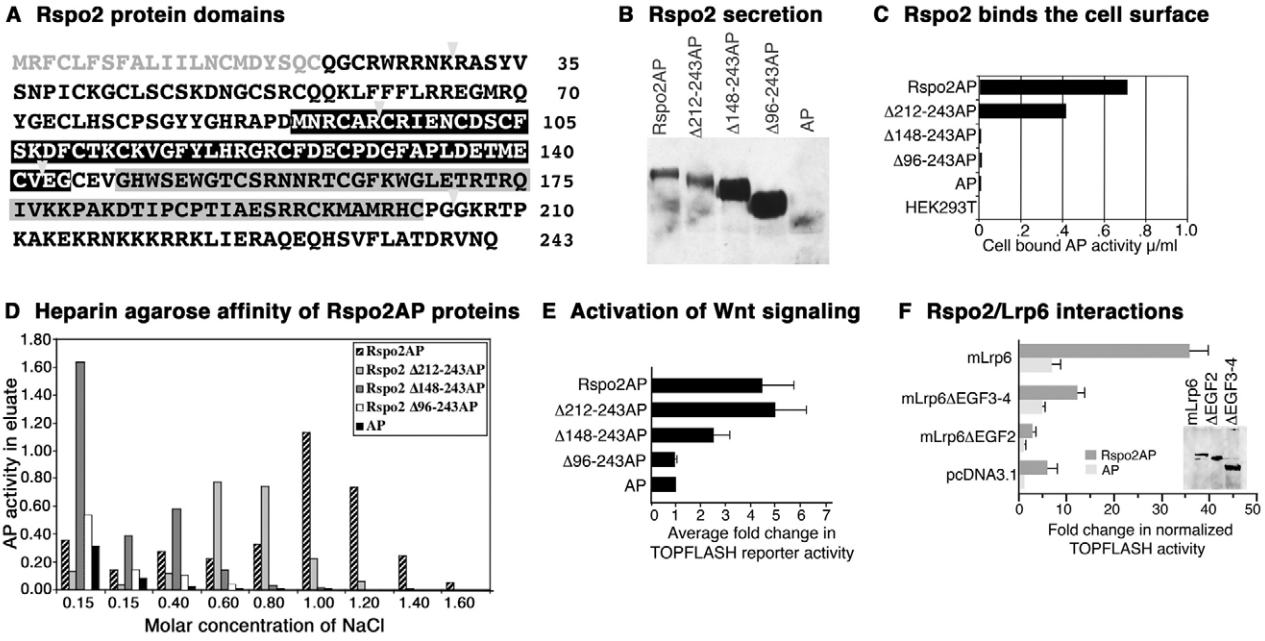

Fig. 2. Structural requirements for activation of Wnt signaling by Rspo2. (**A**) Domains of Rspo2. Signal peptide (light gray) followed by a cysteine-rich domain, a furin-like domain (black box), a TSP1 domain (gray box) and a basic C-terminus. Arrowheads indicate exon junctions. (**B**) Western blot analysis. An anti-AP antibody detected appropriately sized Rspo2AP fusion proteins in concentrated conditioned media. (**C**) Conditioned media containing the indicated Rspo2AP fusion proteins was incubated with untransfected HEK293T cells and cell bound AP activity determined. (**D**) Binding affinity of Rspo2AP fusion products to heparin agarose, only Rspo2AP and Δ212-243AP possessed a high affinity for heparin. (**E**) HEK293T cells co-transfected with TOPFLASH and pRL-TK were exposed to the indicated conditioned media. Firefly luciferase was normalized to *Renilla* luciferase activity. Activity induced in response to AP conditioned media was set to 1. Furin domain-containing constructs activated TOPFLASH. (**F**) Flag-tagged *Lrp6* expression constructs with the indicated domains deleted were co-transfected into HEK293T cells with TOPFLASH and pRL-TK. Normalized luciferase activity in pcDNA3.1-transfected cells exposed to AP conditioned media was set to 1. Bars represent the mean±s.e.m. induction. Inset shows western blot of cell lysates from parallel wells. An anti-flag antibody detected expression of appropriately sized Lrp6 proteins.

Rspo2 and Lrp6 interactions

In HEK293T cells expressing Lrp6, Rspo2 increased Wnt signaling approximately sevenfold (Fig. 2F). The extracellular domain of Lrp6 contains 4 EGF-like domains separated by multiple LDL repeats. To identify the regions within the extracellular domain of Lrp6 that interact with Rspo2, Flag-tagged Lrp6 and deletion mutants lacking either EGF-like domain 2 (ΔEGF2) or 3 and 4 (ΔEGF3-4) were co-transfected with TOPFLASH and pRL-TK into HEK293T cells and then exposed to Rspo2AP or AP conditioned media for 24 hours. TOPFLASH expression was highest in the presence of Rspo2AP and full-length Lrp6. Although ΔEGF3-4 increased TOPFLASH activity in the presence of Rspo2AP, ΔEGF2 was not active (Fig. 2F). Western blot analysis detected appropriately sized Lrp6 proteins in the transfected cells (Fig. 2F insert). Therefore, Rspo2 activation of canonical Wnt signaling is dependent on the second EGF-like domain of Lrp6. The reduction in the level of TOPFLASH activation observed by ΔEGF3-4 suggests that these domains may also be involved in Rspo2 signaling.

Embryonic expression of *Rspo2*

Rspo2 expression in the developing mouse embryo was evaluated at midgestation by in situ hybridization. Antisense riboprobes to various regions of the cDNA resulted in identical expression patterns. *Rspo2* was first observed in the pre-forebrain neural tissue in E8 embryos with 7-10 pairs of somites (data not shown). By E9.5, expression was present within the dorsal forebrain at the forebrain/midbrain junction, the isthmus, ventral ectoderm of the emerging forelimb bud and lung bud (Fig. 3A). Through E10 and E11, *Rspo2* mRNA persisted in the forebrain, isthmus, limb ectoderm and lung, and was detected in the branchial arches, genital ridge and limb mesenchyme (Fig. 3B,D). At E10, a transient stripe of expression was detected at the ventral base of the hindlimb bud (Fig. 3B). Expression of *Rspo2* persisted in the lung bud mesenchyme through E14 and was detected as discrete domains within the laryngeal region from E11.5-15 (Fig. 3F-H, data not shown). Other sites of expression included the cortical hem of the telencephalon (E14), nasal pits and tooth mesenchyme (E15) (Fig. 3E, data not shown). These observations reveal additional sites of expression and are in agreement with previous reports (Kazanskaya et al., 2004; Nam et al., 2007a).

Sp8 is required for expression of *Rspo2* in the AER

Morphogenesis of the AER is dependent upon expression of the transcription factor *Sp8* in the ventral ectoderm of the emerging limb bud (Bell et al., 2003b). Cells initially fated to form the AER are present in the ventral ectoderm of $Sp8^{-/-}$ hindlimb buds, express a variety of AER markers, but fail to form a mature AER (Bell et al., 2003b). *Rspo2* expression was assessed in $Sp8^{-/-}$ embryos since $Rspo2^{Tg/Tg}$ embryos exhibit a disruption in AER maturation (Bell et al., 2003a) and *Rspo2* is coordinately expressed with *Sp8* in the forming and mature AER cells (Fig. 3A,B,D,J,K). *Rspo2* mRNA was not detected in limb buds of E10 $Sp8^{-/-}$ embryos, although expression was present in the telencephalon (Fig. 3C). Real-time RT-PCR determined that the *Rspo2* mRNA level in E10.5 $Sp8^{-/-}$

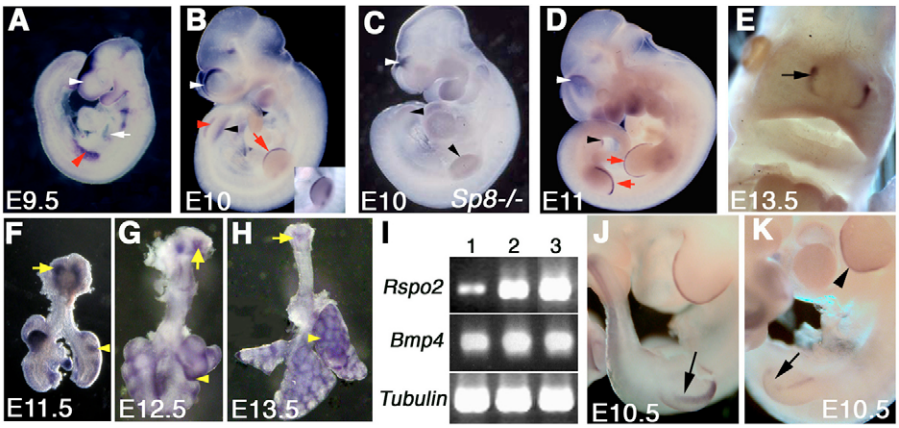

Fig. 3. *Rspo2* expression is regulated by Sp8 in the limb. Whole-mount in situ hybridization was performed on wild-type (A,B,D-H,J), $Sp8^{-/-}$ (C) and $Rspo2^{Tg/Tg}$ (K) embryos of the indicated age [embryonic day (E)]. (A-H) *Rspo2* antisense riboprobe corresponding to sequences in EST AK011587. (J,K) *Sp8* antisense riboprobe. (A-D) Telencephalon expression (white arrowheads). (**A**,**B**) AER precursors (red arrowheads). (B,D) Mature AER (red arrows). (B) Transient domain at base of hindlimb (black arrowhead); inset highlights proximal mesenchymal expression domain. (**C**) *Rspo2* expression is undetectable in limb buds (black arrowheads). (**D**) Genital ridge expression (black arrowhead). (**E**) Expression in nasal pits. (**F-H**) *Rspo2* expression in laryngeal regions (arrows) and lung mesenchyme (arrowheads). (**I**) Real-time RT-PCR products amplified from cDNA prepared from stage 2 hindlimb bud ectoderm from $Sp8^{-/-}$ (lane 1) or $Sp8^{+/+}$ (lane 2), and stage 4 $Sp8^{+/+}$ (lane 3) embryos. *Rspo2* was dramatically decreased in $Sp8^{-/-}$ ectoderm and increased during limb outgrowth in control embryos, whereas the expression of other AER markers was changed less than twofold. (**J**,**K**) Arrows indicate differences in *Sp8* expression in the posterior AER margin; expression is weaker in $Rspo2^{Tg/Tg}$ forelimb AER (arrowhead).

hindlimb ectoderm was reduced eightfold compared with controls (Fig. 3I). The AER markers *Bmp4* and *Dlx2* were reduced only 1.5- to twofold (Fig. 3I, data not shown). As the hindlimb AER matured between stages 1 (Fig. 3B) and 4 (Fig. 3D), *Rspo2* mRNA increased approximately fourfold. Expression of *Bmp4* and *Dlx2* was unchanged (Fig. 3I, data not shown). By contrast, *Sp8* expression was detectable in the fore and hindlimb AERs of $Rspo2^{+/+}$ and $Rspo2^{Tg/Tg}$ embryos (Fig. 3J,K). As previously described (Bell et al., 2003a), AER deficiencies are not readily detectable in E10.5 $Rspo2^{Tg/Tg}$ embryos with fewer than ~35 somites. Like other AER markers, disruptions in *Sp8* expression were observed along the posterior hindlimb and anterior forelimb margins of $Rspo2^{Tg/Tg}$ embryos (Fig. 3K). Notably, *Sp8* expression within the AER containing areas of the $Rspo2^{Tg/Tg}$ fore and hindlimbs appeared weaker. Nam et al. recently reported a similar limb phenotype in fetuses homozygous for a gene targeted *Rspo2* allele and also observed a decrease in *Sp8* expression (Nam et al., 2007b). These observations suggest that *Rspo2* expression is dependent on Sp8 within the AER precursors and support previous observations indicating that continued *Sp8* expression is regulated by canonical Wnt signaling (Bell et al., 2003b; Kawakami et al., 2004).

Developmental roles of Rspo2

To test whether Rspo2 activation of the canonical Wnt signaling pathway was influenced by Lrp6 in vivo, the limb phenotypes were assessed in progeny with varying doses of each allele. The data presented in Table S1 in the supplementary material indicates the frequency of missing skeletal elements observed by genotype. $Rspo2^{Tg/Tg};Lrp6^{+/+}$ fetuses exhibited a 38% incidence of right forelimb ectrodactyly 1 and/or 2 (Fig. 4A) (Bell et al., 2003a). Forelimb ectrodactyly 5 was a characteristic of $Rspo2^{+/+};Lrp6^{-/-}$ fetuses (99%) (Pinson et al., 2000) and was also observed in the right forelimb of $Rspo2^{+/Tg};Lrp6^{+/-}$ animals (~20%) (Fig. 4B,D; see Table S1 in the supplementary material). An increase in the number of progeny missing digits and with malformations of more proximal skeletal elements was observed in $Rspo2^{Tg/Tg};Lrp6^{+/-}$ and $Rspo2^{+/Tg};Lrp6^{-/-}$ mice (Fig. 4C,E). $Rspo2^{Tg/Tg};Lrp6^{-/-}$ fetuses lacked all forelimb skeletal elements and had scapular malformations (Fig. 4F).

Severe malformations of the hindlimb, including loss of the autopod and fibula were observed in $Rspo2^{Tg/Tg}$ fetuses (Fig. 4G) (Bell et al., 2003a). Similarly, *Lrp6* homozygotes lacked the autopod and fibula (100% penetrant) and possessed malformations of the tibia (52%) and femur (24%) (Fig. 4H) (Pinson et al., 2000). $Rspo2^{Tg/Tg};Lrp6^{+/-}$ mice exhibited a higher incidence of tibia and femur defects (Fig. 4I). Reciprocally, $Rspo2^{+/Tg};Lrp6^{-/-}$ fetuses consistently lacked both autopods and all or most of the tibia and fibula. Additionally, an increase in the severity of femur and pelvic girdle malformations was observed (compare Fig. 4K with 4H). No hindlimb structures and only rudiments of the pelvic girdle were observed in $Rspo2^{Tg/Tg};Lrp6^{-/-}$ progeny (Fig. 4L). A few $Rspo2^{+/Tg};Lrp6^{+/-}$ fetuses lacked digits (Fig. 4J).

Rspo2 and Lrp6 influence laryngeal-tracheal morphogenesis

Malformations in laryngeal and tracheal cartilages of E18 $Rspo2^{Tg/Tg}$ fetuses were observed and exacerbated by the progressive loss of *Lrp6* alleles. The laryngeal region consists of the hyoid bone and thyroid, arytenoid and cricoid cartilages. In $Rspo2^{+/+}$ or $^{+/Tg}$ animals, regardless of *Lrp6* genotype, the arytenoid cartilages floated freely above the cricoid cartilage. These cartilages were usually fused to the top of the cricoid in $Rspo2^{Tg/Tg};Lrp6^{+/+}$ and $Rspo2^{Tg/Tg};Lrp6^{+/-}$ fetuses (Fig. 5B-D; see Table S2 in the supplementary material). The cricoid normally forms a thickened ring with a dorsal region of cartilage that extends caudally. The cricoid ring was not formed in $Rspo2^{Tg/Tg}$ fetuses and the dorsal aspect of the cricoid was absent (Fig. 5A-C). In $Rspo2^{+/+};Lrp6^{+/+}$and $Rspo2^{+/Tg};Lrp6^{+/+}$ progeny, 12-15 tracheal rings were evenly spaced with one or two bifurcated rings. Defects in cartilage ring formation varied from normal to bifurcated or consisted of abnormal cartilaginous nodules within the

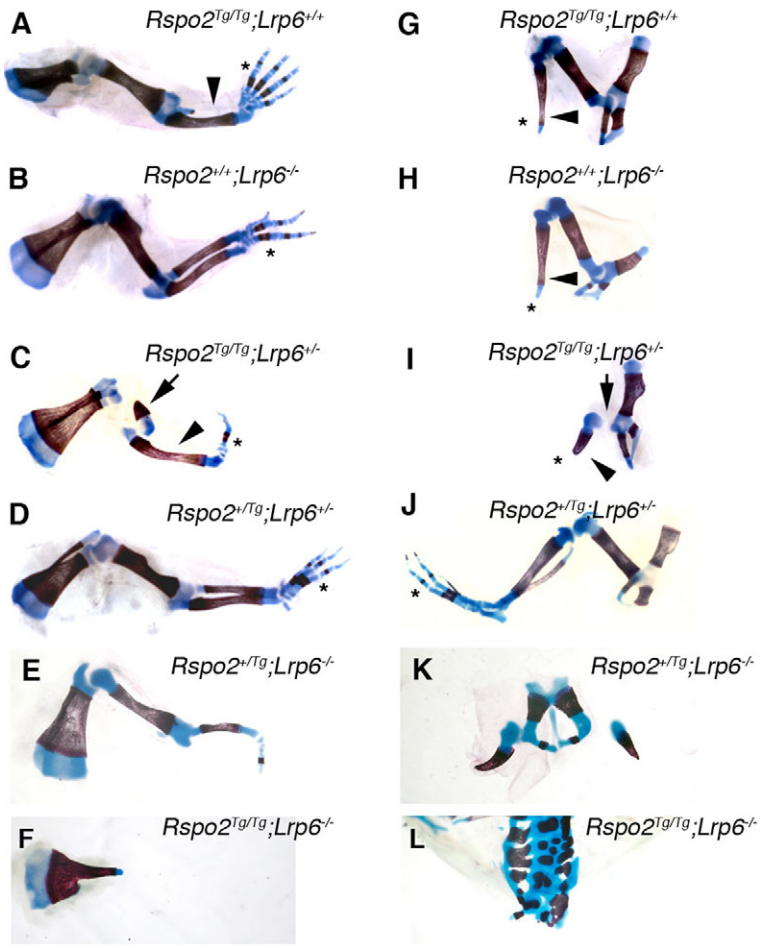

Fig. 4. Rspo2 and Lrp6 interact during morphogenesis of the limbs. Alcian Blue and Alizarin Red stained E18.5 right forelimbs (**A-F**) and left hindlimbs (**G-L**). Asterisks in A-D and G-J indicate absence of digits. Arrowheads in A and C indicate absence of a radius. Arrow in C indicates malformation of the humerus. Arrowhead in G-I indicate absence of the fibula. Arrow in I indicates absence of the femur.

trachea and mainstem bronchi in $Rspo2^{Tg/Tg};Lrp6^{+/+}$ and $Rspo2^{Tg/Tg};Lrp6^{+/-}$ mice (Fig. 5B,C). A severe phenotype was observed in $Rspo2^{Tg/Tg};Lrp6^{-/-}$ fetuses; only rudiments of the thyroid cartilage were present and tracheal rings were absent (Fig. 5D). Laryngeal and tracheal cartilages were normal in $Rspo2^{+/+};Lrp6^{-/-}$ and $Rspo2^{+/Tg};Lrp6^{-/-}$ fetuses (Fig. 5E). Supporting the hypothesis that Rspo2 signals to the airway epithelium and acts through the canonical Wnt signaling pathway, tracheal ring defects were observed in doxycycline-exposed *Tg(SFPTC-rtTA)*5Jaw^{+};*Tg(TetO7-CMVcre)*$^{+}$;*β-catenin*$^{flox/flox}$ mice (Mucenski et al., 2003) in which *β-catenin* was conditionally deleted from the embryonic airway epithelium (Fig. 5F, see Table S3 in the supplementary material).

Rspo2 and Lrp6 influence lung growth and morphogenesis

$Rspo2^{Tg/Tg}$ mice die immediately after birth. As *Rspo2* mRNA was observed in the lung bud mesenchyme, lung morphogenesis was assessed in $Rspo2^{Tg/Tg}$ embryos. Fetal weights and crown-rump lengths varied by genotype, owing to the limb malformations and presence of spina bifida in $Lrp6^{-/-}$ fetuses. Therefore, lung weights were normalized to fetal body circumferences, Table 1. As noted for the laryngeal and tracheal cartilages, lung size was normal in $Rspo2^{+/+};Lrp6^{-/-}$ and $Rspo2^{+/Tg};Lrp6^{+/-}$ progeny. An ~50% or more reduction in normalized lung weight was observed in $Rspo2^{Tg/Tg};Lrp6^{+/+}$, $Rspo2^{Tg/Tg};Lrp6^{+/-}$, $Rspo2^{Tg/Tg};Lrp6^{-/-}$ and $Rspo2^{+/Tg};Lrp6^{-/-}$ fetuses, all statistically significant at $P<0.05$. Although the right lung lobes of $Rspo2^{Tg/Tg}$ mice were frequently fused proximally, the overall lung structure and was not substantially altered. Immunohistochemical staining for specific cell types using antibodies to pro-surfactant protein C (type II epithelial cells), FoxJ1 (ciliated epithelial cells), Pecam1 (vascular endothelial cells), T1-alpha (type I epithelial cells), alpha-smooth muscle actin (smooth muscle cells) and Clara cell secretory protein (nonciliated bronchiolar cells) indicated that the expected differentiation of the various pulmonary cell types had occurred in lungs of all genotypes (Fig. 5G-N; see Fig. S2 in the supplementary material, data not shown). Thus, the hypoplasia observed in $Rspo2^{Tg/Tg};Lrp6^{+/+}$ and $Rspo2^{Tg/Tg};Lrp6^{-/-}$ animals did not correlate with the absence of a specific population of differentiated cells in the E18.5 lung.

To determine the timing of lung malformations, lung buds were dissected from E11.5-15.5 embryos. As early as E11.5, the number of epithelial branches was reduced in $Rspo2^{Tg/Tg}$ mice and these defects persisted throughout embryogenesis, as highlighted by *Sox9* staining at E13 (Fig. 6; Fig. 7A-C,E,G,H). Lung buds isolated from E11.5 $Rspo2^{Tg/Tg}$ and nonmutant littermates were cultured in the presence of conditioned media containing either AP or Rspo2 Δ212-243AP, and terminal epithelial tips were counted after 3 days in organ culture. Confirming a defect in branching morphogenesis, the branching of $Rspo2^{Tg/Tg}$ lung buds in AP medium was significantly reduced compared with controls, $P<0.001$ by two-tailed Student's *t*-test (compare Fig. 6A with 6C). This defect was substantially rescued by culturing $Rspo2^{Tg/Tg}$ lung buds in media containing Rspo2 Δ212-243AP, $P<0.001$ (Fig. 6A,B). Within individual experiments, similar levels of branching were observed in $Rspo2^{+/+}$ and $Rspo2^{+/Tg}$ lung buds exposed to Rspo2 Δ212-243AP or AP (Fig. 6C,D).

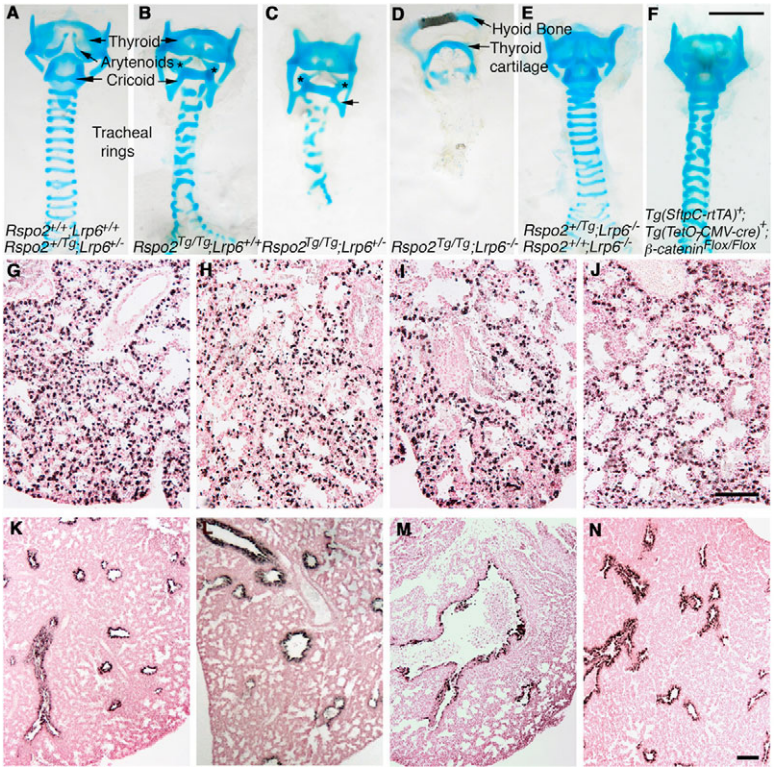

Fig. 5. Laryngeal-tracheal-bronchial and lung malformations in *Rspo2/Lrp6* mutant mice. (**A-F**) Alcian Blue stained cartilages in the larynx, trachea and bronchi from E18.5 fetuses of indicated genotypes. Asterisks in B and C indicate fusion of the arytenoids to the cricoid cartilage. (C) Arrow indicates the cricoid; cartilage is absent on the dorsal aspect of the ring, also observed in B and D. (F) The *SftpC-rtTA* transgene does not target cells within the larynx epithelium and only tracheal ring defects were observed. (**G-N**) Immunohistochemical analysis for pro-SftpC, a type II epithelial cell marker (G-J); and Ccsp, a nonciliated bronchiolar cell marker (K-N). (G,K) $Rspo2^{+/+};Lrp6^{+/+}$; (H,L) $Rspo2^{Tg/Tg};Lrp6^{+/+}$; (I,M) $Rspo2^{Tg/Tg};Lrp6^{-/-}$; (J,N) $Rspo2^{+/+};Lrp6^{-/-}$. Scale bars: 1 mm in F; 10 μm in J and N.

To determine whether *Rspo2* deficiency influenced canonical Wnt signaling during embryogenesis, the TOPGAL reporter transgene (DasGupta and Fuchs, 1999) was mated into the $Rspo2^{Tg}$ line. In E11.5 $Rspo2^{Tg/Tg};TOPGAL^{+/-}$ lung buds, the normal pattern of TOPGAL activity was disrupted; staining was decreased at the distal tips of the branching epithelium (compare Fig. 7A with 7B,C,E). A statistically significant difference in the amount of TOPGAL signaling was found by assaying protein concentration and β-galactosidase activity in individual E11.5 wild-type and $Rspo2^{Tg/Tg}$ lung buds ($P<0.00002$ by two-tailed Student's *t*-test of unequal variance) (Fig. 7D). Real-time RT-PCR of E11.5 lung cDNA samples evaluated the expression of the Wnt downstream target genes *Lef1* and *Irx3* (Braun et al., 2003; Hovanes et al., 2001), both expressed by the lung epithelium (De Langhe et al., 2005; Houweling et al., 2001). *Fgf10* expression was also examined owing to its known role in branching morphogenesis (Bellusci et al., 1997). *Irx3* expression was decreased threefold in $Rspo2^{Tg/Tg}$ lung buds, consistent with its proposed role in branching morphogenesis (van Tuyl et al., 2006) (Fig. 7F). *Lef1* and *Fgf10* expression varied between the two $Rspo2^{Tg/Tg}$ samples but were decreased less than 1.5-fold. These observations are consistent with the concept that Rspo2 is involved in activation of canonical Wnt signaling in the embryonic lung.

Taken together, these observations support the concept that *Rspo2* is required for normal branching morphogenesis and growth of the embryonic lung, but is not required for cephalo-caudal patterning of the respiratory tract or differentiation of epithelial and mesenchymal cell types.

DISCUSSION

We have shown that the insertional mutation *footless* creates a severe mutation in the *Rspo2* gene. In vitro, Rspo2-AP activated canonical Wnt signaling while Rspo2 deficiency reduced Wnt signaling in the embryonic respiratory tract, as indicated by in vivo TOPGAL expression. The $Rspo2^{Tg}$ allele caused severe malformations of the hindlimb, larynx, trachea, bronchi and lungs that were exacerbated by reduction in Lrp6.

Table 1. E18.5 fetal lung weights

Genotype	Number of litters	Number of fetuses	Average lung weight (g±s.e.m.)	Average body circumference (cm±s.e.m.)	Average lung weight/body circumference
$Rspo2^{+/+};Lrp6^{+/+}$	12	17	0.038±0.0003	2.43±0.0104	0.0157±0.0001
$Rspo2^{+/Tg};Lrp6^{+/+}$	8	12	0.040±0.0005	2.46±0.0067	0.0160±0.0001
$Rspo2^{+/Tg};Lrp6^{+/-}$	11	20	0.036±0.0002	2.39±0.0067	0.0149±0.0001
$Rspo2^{+/Tg};Lrp6^{-/-}$	9	11	0.028±0.0007	2.20±0.0167	0.0125±0.0002*
$Rspo2^{Tg/Tg};Lrp6^{+/+}$	11	16	0.022±0.0003	2.52±0.0090	0.0085±0.0001*
$Rspo2^{Tg/Tg};Lrp6^{+/-}$	8	13	0.016±0.0004	2.18±0.0250	0.0074±0.0002*
$Rspo2^{Tg/Tg};Lrp6^{-/-}$	2	2	0.002±0.0007	2.10±0.0707	0.0010±0.0004*
$Rspo2^{+/+};Lrp6^{+/-}$	13	19	0.041±0.0003	2.51±0.0087	0.0163±0.0001
$Rspo2^{+/+};Lrp6^{-/-}$	6	10	0.032±0.0003	2.25±0.0158	0.0141±0.0002

*Statistically significant by one-way ANOVA, $P<0.05$.

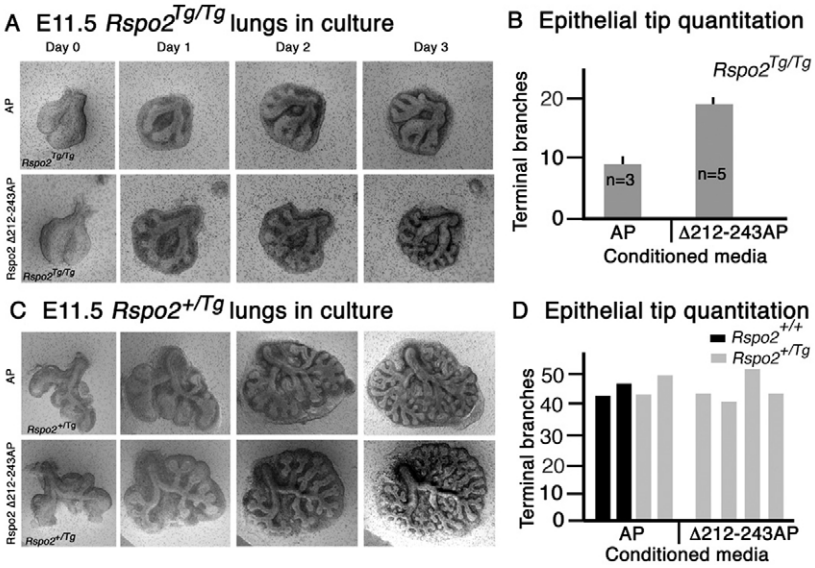

Fig. 6. Branching defects in *Rspo2*$^{Tg/Tg}$ lungs. Organ culture of E11.5 lungs in the presence of conditioned media containing either AP or Rspo2 Δ212-243AP. (**A**) Rspo2 Δ212-243AP partially rescued the branching defect observed in *Rspo2*$^{Tg/Tg}$ lung buds. (**B**) Counted epithelial tips of mutant lung buds in culture. (**C**,**D**) *Rspo2*$^{+/+}$ and *Rspo2*$^{+/Tg}$ lung buds grew similarly in culture in response to either AP or Rspo2 Δ212-243AP. (D) Number of distal tips of individual lung buds observed within a representative experiment.

In vitro evidence indicates that Rspo binding to Lrp6 activates canonical Wnt signaling. In the present studies, Rspo2 increased TOPFLASH activity in response to increasing levels of cellular Lrp6, consistent with previous studies (Kazanskaya et al., 2004; Nam et al., 2006). Rspo1 and Rspo3 have been co-immunoprecipitated with the extracellular domain of Lrp6 (Nam et al., 2006; Wei et al., 2007). Herein, we observed that the second Lrp6 EGF-like repeat was required for Rspo2 activation of canonical Wnt signaling, whereas some signaling was retained in the absence of EGF-like repeats 3 and 4. Prior studies using human Lrp6 constructs demonstrated that EGF-like domains 1 and 2 were required for binding to Wnts and Wise (Itasaki et al., 2003; Mao et al., 2001). As the cellular response to Wnts is increased in the presence of Rspo2, it is unclear whether Rspo2 competes with Wnts for binding to the EGF 1 and 2 domains on the same Lrp6 molecule or whether a Wnt ligand binds to one EGF domain and Rspo2 to the other to activate signaling. The higher affinity of Rspo proteins for Lrp6, when compared with frizzled proteins, may indicate that they bind in a larger complex, with Lrp6-Rspo2 interacting with a Wnt-frizzled (Wei et al., 2007). Alternatively, the effects of ligand binding to frizzled or Lrp6 receptors may activate shared downstream targets independently.

Morphogenetic defects caused by deletion of *Rspo2* or *Lrp6* alone were exacerbated by decreasing the dosage of the other gene. These findings support the concept that Rspo2 and Lrp6 function in a shared/overlapping pathway affecting formation of the limb and respiratory tract. *Rspo2*$^{Tg/Tg}$*;Lrp6*$^{-/-}$ fetuses lacked appendages. Defects in the pelvic and shoulder girdles of *Rspo2*$^{Tg/Tg}$*;Lrp6*$^{-/-}$ mice are probably related to the absence of *Rspo2* expression in the most proximal mesenchyme of the emerging limb bud, as formation of these structures is independent of AER formation (Sun et al., 2002). By contrast, the progressive loss of distal limb structures in *Rspo2*$^{Tg/Tg}$*;Lrp6*$^{+/+}$ and *Rspo2*$^{Tg/Tg}$*;Lrp6*$^{+/-}$ or *Rspo2*$^{+/+}$*;Lrp6*$^{-/-}$ and *Rspo2*$^{+/Tg}$*;Lrp6*$^{-/-}$ is probably related to the progressive loss of AER. Both Lrp6 and Rspo2 mutants are known to affect AER morphogenesis (Bell et al., 2003a; Pinson et al., 2000) and the AER is required for outgrowth of the underlying mesenchyme. The importance of Rspo2 for normal AER morphogenesis is supported by the observations that *Rspo2* expression increased as the AER matured and that it was dramatically decreased in *Sp8*$^{-/-}$ limb buds that fail to form an AER (Bell et al., 2003b). The highest levels of canonical Wnt signaling colocalize in the pre and mature AER cells where *Rspo2* is expressed (Barrow et al., 2003; Maretto et al., 2003). Notably, *Wnt3* and *Lrp6* both are expressed throughout the limb

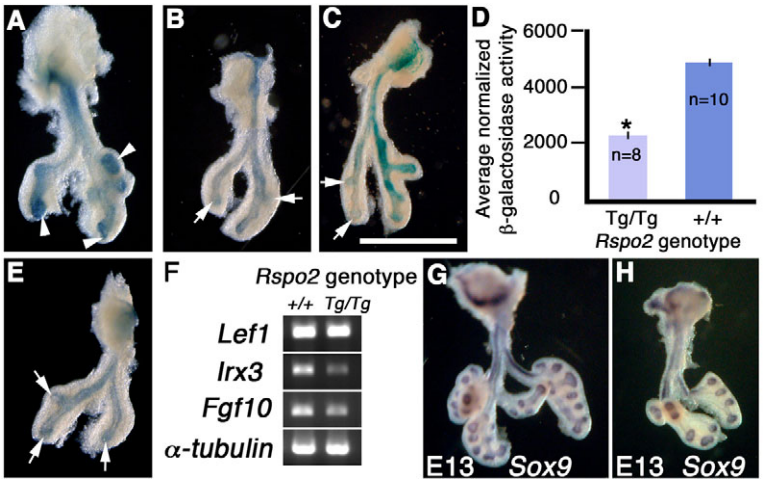

Fig. 7. *Rspo2*$^{Tg/Tg}$ lungs exhibit reduced Wnt signaling. The *Rspo2*^{Tg} allele was crossed into the Wnt signaling reporter TOPGAL line and β-galactosidase activity examined in whole-mount lung specimens at E11.5: *Rspo2*$^{+/+}$ (**A**), *Rspo2*$^{Tg/Tg}$ (**B**,**C**,**E**). A, B and E are littermates. White arrows indicate high levels of Wnt signaling activity in the distal tips of wild-type lungs compared with the lower level in the distal tips of mutants (arrowheads). (**D**) Quantitation of β-galactosidase activity in E11.5 lung buds. (**F**) Semi-quantitative real-time RT-PCR of E11.5 cDNA samples, indicating that *Irx3* is reduced threefold. (**G**,**H**) *Sox9* is expressed in a normal proximal distal pattern in *Rspo2*$^{+/+}$ (G) and *Rspo2*$^{Tg/Tg}$ (H) lungs.

ectoderm and, together with β-catenin, are required for normal AER morphogenesis (Barrow et al., 2003; Pinson et al., 2000). We propose a model in which Rspo2 in the AER enhances canonical Wnt signaling to a level necessary for normal limb morphogenesis. This process is tightly regulated as the AER simultaneously expresses the Wnt signaling antagonist Dickkopf 1 (*Dkk1*) (Mukhopadhyay et al., 2001). An overactive AER is present in *Dkk1* mutants, resulting in limbs with extra digits. Notably, in the absence of *Dkk1*, reduction of either *Lrp5* or *Lrp6* expression lowers the incidence of limb malformations (MacDonald et al., 2004).

The morphogenetic defects present in $Rspo2^{Tg/Tg}$ included severe malformations of the larynx, trachea, bronchi and lung. At E18.5, $Rspo2^{Tg/Tg}$ fetal lungs were approximately half the size of littermate lungs but generally retained normal structure and cephalo-caudal patterning of differentiated cell types. Laryngeal and tracheal-bronchial ring abnormalities were observed in all $Rspo2^{Tg/Tg}$ fetuses and included malformation of the cricoid ring and arytenoids within the larynx, and absent or malformed cartilage rings in the trachea and bronchi. *Lrp6* heterozygosity did not increase the severity of these $Rspo2^{Tg/Tg}$ malformations, suggesting that other Rspos or Wnts can compensate in the absence of Rspo2. The lack of tracheal and laryngeal defects in $Rspo2^{+/+}$;$Lrp6^{-/-}$ and $Rspo2^{+/Tg}$;$Lrp6^{-/-}$ fetuses suggests that in the absence of Lrp6, Rspo2 may signal through Lrp5. Like Lrp6, Lrp5 can mediate canonical Wnt signaling but, surprisingly, loss of Lrp5 is compatible with life (Holmen et al., 2004; Mikels and Nusse, 2006). The dramatic effect of the Rspo2 mutation on lung growth and laryngeal-tracheal-bronchial morphogenesis observed in $Rspo2^{Tg/Tg}$;$Lrp6^{-/-}$ mice indicates a critical requirement for early Lrp6-mediated Rspo2 signaling. The finding that deletion of β-catenin from the embryonic respiratory epithelium also resulted in tracheal ring malformations supports a role of Rspo2-mediated activation of the canonical Wnt signaling pathway in tracheal cartilage morphogenesis.

During early lung formation, canonical Wnt signaling is highest in the distal lung epithelium and immediately adjacent mesenchyme (De Langhe et al., 2005). At E11.5, a reduction in expression of the Wnt signaling reporter TOPGAL was observed in distal epithelial tips of $Rspo2^{Tg/Tg}$ lung buds with a defect in epithelial branching. As *Rspo2* is expressed in the distal tip mesenchyme, we propose that paracrine Rspo2 signaling occurs in the lung. In support of this concept, the highest levels of *Lrp6* and *Lrp5* expression are observed in the respiratory epithelium that also expresses *Wnt7b*, *Wnt5a*, *Wnt11*, *Fzd8* and *Fzd10* (De Langhe et al., 2005; Li et al., 2002). *Wnt2a*, *Wnt5a*, *Wnt11*, *Fzd1*, *Fzd4* and *Fzd7* are expressed in the lung mesenchyme (Li et al., 2002; Wang et al., 2005; Weidenfeld et al., 2002). In vitro studies demonstrated R-spondin activation of the canonical Wnt pathway through interactions with Lrp6 and Fzd1, Fzd4, Fzd5 and Fzd8, as well as potentiation of Wnt1 and Wnt3a signaling (Kazanskaya et al., 2004; Nam et al., 2006; Wei et al., 2007; Weidenfeld et al., 2002). Whether Rspo2 acts independently or potentiates the canonical signaling activity of Wnt7b, Wnt5a, Wnt2 or Wnt11 in the lung remains to be determined (Mikels and Nusse, 2006). Wnt7b signaling is thought to be dependent on interactions with Lrp5, Fzd1 and Fzd10 (Wang et al., 2005). The early branching defects and lung hypoplasia observed in $Rspo2^{Tg/Tg}$ embryos, were similar to those observed in *Wnt7b* mutants. However, epithelial cell differentiation proceeded normally in $Rspo2^{Tg/Tg}$ mice, whereas $Wnt7b^{-/-}$ mice exhibited a deficiency in type I cell differentiation (Shu et al., 2002).

The distinct combination of tracheal malformations and lung hypoplasia observed in $Rspo2^{Tg/Tg}$ mice is reminiscent of other genetic mutations. Retinoic acid receptor (Rar) $\alpha^{-/-}\beta2^{-/-}$ animals exhibit lung hypoplasia attributable to a delay in branching morphogenesis that was detectable as early as E11.5 (Mendelsohn et al., 1994). Laryngeal and tracheal defects in $Rar\alpha^{-/-}Rar\beta2^{-/-}$ fetuses also included failure of the cricoid to fuse dorsally, fusion of the arytenoids to the cricoid, and abnormally shaped cartilage rings. By contrast, the foreshortening of the trachea seen in $Rar\alpha^{-/-}Rar\beta2^{-/-}$ was not observed in $Rspo2^{Tg/Tg}$ mice. Abnormally formed tracheal-bronchial rings were also observed after conditional deletion of *Shh* in the respiratory epithelium (Miller et al., 2004). By contrast, the tracheal cartilage abnormalities found in *Wnt5a* and TNF receptor-associated factor 4 (*Traf4*)-null mice are distinct. In $Wnt5a^{-/-}$ mice, tracheal length was shorter but the tracheal rings were normal (Li et al., 2002). The upper three to six cartilage rings below the cricoid were consistently either frontally disrupted or fused in $Traf4^{-/-}$ fetuses (Regnier et al., 2002; Shiels et al., 2000). The role of Rspo2 in this developmental process is currently unclear.

In summary, the *footless* insertional mutation disrupts the *Rspo2* gene, causing severe malformations in the lung, larynx, trachea, bronchi, limb and palate. The restricted sites of *Rspo2* expression correlated with the sites of malformation. The effects of the *Rspo2* mutation on morphogenesis is distinct from those associated with mutations of other R-spondin family members. Deletion of *Rspo3* resulted in embryo lethality at E10 that was attributed to impaired placentation (Aoki et al., 2007). *RSPO1* mutations were associated with XX sex reversal, palmoplantar hyperkeratosis and a predisposition to squamous cell carcinoma (Parma et al., 2006). *RSPO4* mutations result in anonychia (Blaydon et al., 2006), consistent with the finding that *Rspo4* is selectively expressed in the nail bed. The present studies indicate that Rspo2 and Lrp6 interact to activate canonical Wnt signaling affecting limb and laryngeal-tracheal cartilages, and lung morphogenesis.

This work was supported in part by National Institutes of Health Grant HD-24517 to W.J.S. and HL-75770, HL090156, and HL61646 to J.A.W. We would like to thank members of the Pulmonary Biology Morphology Core for technical assistance.

Supplementary material

Supplementary material for this article is available at
http://dev.biologists.org/cgi/content/full/135/6/1049/DC1

References

Aoki, M., Mieda, M., Ikeda, T., Hamada, Y., Nakamura, H. and Okamoto, H. (2007). R-spondin3 is required for mouse placental development. *Dev. Biol.* **301**, 218-226.

Barrow, J. R., Thomas, K. R., Boussadia-Zahui, O., Moore, R., Kemler, R., Capecchi, M. R. and McMahon, A. P. (2003). Ectodermal Wnt3/β-catenin signaling is required for the establishment of the apical ectodermal ridge. *Genes Dev.* **17**, 394-409.

Bell, S. M., Schreiner, C. M., Hess, K. A., Anderson, K. P. and Scott, W. J. (2003a). Asymmetric limb malformations in a new transgene insertional mutant, *footless*. *Mech. Dev.* **120**, 597-605.

Bell, S. M., Schreiner, C. M., Waclaw, R. R., Campbell, K., Potter, S. S. and Scott, W. J., Jr (2003b). *Sp8* is crucial for limb outgrowth and neuropore closure. *Proc. Natl. Acad. Sci. USA* **100**, 12195-12200.

Bell, S. M., Schreiner, C. M., Goetz, J. A., Robbins, D. J. and Scott, W. J. J. (2005). Shh signaling in limb bud ectoderm: Potential role in teratogen-induced postaxial ectrodactyly. *Dev. Dyn.* **233**, 313-325.

Bellusci, S., Grindley, J., Emoto, H., Itoh, N. and Hogan, B. L. (1997). Fibroblast growth factor 10 (FGF10) and branching morphogenesis in the embryonic mouse lung. *Development* **124**, 4867-4878.

Blaydon, D. C., Ishii, Y., O'Toole, E. A., Unsworth, H. C., Teh, M.-T., Ruschendorf, F., Sinclair, C., Hopsu-Havu, V. K., Tidman, N., Moss, C. et al. (2006). The gene encoding R-spondin 4 (*RSPO4*), a secreted protein implicated in Wnt signaling, is mutated in inherited anonychia. *Nat. Genet.* **38**, 1245-1247.

Braun, M. M., Etheridge, A., Bernard, A., Robertson, C. P. and Roelink, H. (2003). Wnt signaling is required at distinct stages of development for the induction of the posterior forebrain. *Development* **130**, 5579-5587.

DasGupta, R. and Fuchs, E. (1999). Multiple roles for activated LEF/TCF transcription complexes during hair follicle development and differentiation. *Development* **126**, 4557-4568.
De Langhe, S. P., Sala, F. G., Del Moral, P. M., Fairbanks, T. J., Yamada, K. M., Warburton, D., Burns, R. C. and Bellusci, S. (2005). Dickkopf-1 (Dkk1) reveals that fibronectin is a major target of Wnt signaling in branching morphogenesis of the mouse embryonic lung. *Dev. Biol.* **277**, 316-331.
Feinstein, Y., Borrell, V., Garcia, C., Burstyn-Cohen, T., Tzarfaty, V., Frumkin, A., Nose, A., Okamoto, H., Higashijima, S., Soriano, E. et al. (1999). F-spondin and mindin: two structurally and functionally related genes expressed in the hippocampus that promote outgrowth of embryonic hippocampal neurons. *Development* **16**, 3637-3648.
Galceran, J., Farinas, I., Depew, M. J., Clevers, H. and Grosschedl, R. (1999). *Wnt3a*$^{-/-}$ -like phenotype and limb deficiency in *Lef1*$^{-/-}$*Tcf1*$^{-/-}$ mice. *Genes Dev.* **13**, 709-717.
Holmen, S. L., Giambernardi, T. A., Zylstra, C. R., Buckner-Berghuis, B. D., Resau, J. H., Hess, J. F., Glatt, V., Bouxsein, M. L., Ai, M., Warman, M. L. et al. (2004). Decreased BMD and limb deformities in mice carrying mutations in both *Lrp5* and *Lrp6*. *J. Bone Miner. Res.* **19**, 2033-2040.
Houck, K. A., Leung, D. W., Rowland, A. M., Winer, J. and Ferrara, N. (1992). Dual regulation of vascular endothelial growth factor bio-availability by genetic and proteolytic mechanisms. *J. Biol. Chem.* **267**, 26031-26037.
Houweling, A. C., Dildrop, R., Peters, T., Mummenhoff, J., Moorman, A. F., Ruther, U. and Christoffels, V. M. (2001). Gene and cluster specific expression of the Iroquois family members during mouse development. *Mech. Dev.* **107**, 169-174.
Hovanes, K., Li, T. W., Munguia, J. E., Truong, T., Milovanovic, T., Marsh, J. L., Holcombe, R. F. and Waterman, M. L. (2001). Beta-catenin-sensitive isoforms of lymphoid enhancer factor-1 are selectively expressed in colon cancer. *Nat. Genet.* **28**, 53-57.
Itasaki, N., Jones, M., Mercurio, S., Rowe, A., Domingos, P. M., Smith, J. C. and Krumlauf, R. (2003). Wise, a context-dependent activator and inhibitor of Wnt signaling. *Development* **130**, 4295-4305.
Kawakami, Y., Esteban, C. R., Matsui, T., Rodriguez-Leon, J., Kato, S. and Izpisua Belmonte, J. C. (2004). *Sp8* and *Sp9*, two closely related buttonhead-like transcription factors, regulate *Fgf8* expression and limb outgrowth in vertebrate embryos. *Development* **131**, 4763-4774.
Kazanskaya, O., Glinka, A., del Barco Barrantes, I., Stannek, P., Niehrs, C. and Wu, W. (2004). R-spondin2 is a secreted activator of Wnt/β-catenin signaling and is required for *Xenopus* myogenesis. *Dev. Cell* **7**, 525-534.
Kilpelainen, I., Kaksonen, M., Kinnunen, T., Avikainen, H., Fath, M., Linhardt, R. J., Raulo, E. and Rauvala, H. (2000). Heparin-binding growth associated molecule contains two heparin-binding β-sheet domains that are homologous to the thrombospondin type I repeat. *J. Biol. Chem.* **275**, 13564-13570.
LaRochelle, W. J., May-Siroff, M., Robbins, K. C. and Aaronson, S. A. (1991). A novel mechanism regulating growth factor association with the cell surface: identification of a PDGF retention domain. *Genes Dev.* **5**, 1191-1199.
Li, C., Xiao, J., Hormi, K., Borok, Z. and Minoo, P. (2002). Wnt5a participates in distal lung morphogenesis. *Dev. Biol.* **248**, 68-81.
Logan, C. Y. and Nusse, R. A. (2004). The Wnt signaling pathway in development and disease. *Annu. Rev. Cell Dev. Biol.* **20**, 781-810.
Lowther, W., Wiley, K., Smith, G. H. and Callahan, R. (2005). A new common integration site, Int7, for Mouse Mammary Tumor virus in mouse mammary tumors identifies a gene whose product has furin-like and thrombospondin-like sequences. *J. Virol.* **79**, 10093-10096.
MacDonald, B. T., Adamska, M. and Meisler, M. H. (2004). Hypomorphic expression of *Dkk1* in the *doubleridge* mouse: dose dependence and compensatory interactions with *Lrp6*. *Development* **131**, 2543-2552.
Mao, B., Wu, W., Li, Y., Hoppe, D., Stannek, P., Glinka, A. and Niehrs, C. (2001). LDL-receptor-related protein 6 is a receptor for Dickkopf proteins. *Nature* **411**, 321-325.
Maretto, S., Cordenonsi, M., Dupont, S., Braghetta, P., Broccoli, V., Hassan, B. A., Volpin, D., Bressan, G. M. and Piccolo, S. (2003). Mapping Wnt/β-catenin signaling during mouse development and in colorectal tumors. *Proc. Natl. Acad. Sci. USA* **100**, 3299-3304.
Mendelsohn, C., Lohnes, D., Decimo, D., Lufkin, T., LeMeur, M., Chambon, P. and Mark, M. (1994). Function of the retinoic acid receptors (RARs) during development. *Development* **120**, 2749-2771.
Mikels, A. J. and Nusse, R. (2006). Purified Wnt5a protein activates or inhibits β-catenin-TCF signaling depending on receptor context. *PLOS Biol.* **4**, e115.
Miller, L. D., Wert, S. E., Clark, J. C., Xu, Y., Perl, A.-K. T. and Whitsett, J. A. (2004). Role of *Sonic hedgehog* in patterning of tracheal-bronchial cartilage and the peripheral lung. *Dev. Dyn.* **231**, 57-71.
Mucenski, M. L., Wert, S. E., Nation, J. M., Loudy, D. E., Huelsken, J., Birchmeier, W., Morrisey, E. E. and Whitsett, J. A. (2003). Beta-catenin is required for specification of proximal/distal cell fate during lung morphogenesis. *J. Biol. Chem.* **278**, 40231-40238.
Mukhopadhyay, M., Shtrom, S., Rodriguez-Esteban, C., Chen, L., Tsuki, T., Gomer, L., Dorard, D. W., Glinka, A., Grinberg, A., Huang, S. P. et al. (2001). Dickkopf1 is required for embryonic head induction and limb morphogenesis in the mouse. *Dev. Cell* **1**, 423-434.
Nam, J.-S., Turcotte, T. J., Smith, P. F., Choi, S. and Yoon, J. K. (2006). Mouse Cristin/R-spondin family proteins are novel ligands for the Frizzled8 and Lrp6 receptors and activate β-catenin-dependent gene expression. *J. Biol. Chem.* **281**, 13247-13257.
Nam, J.-S., Turcotte, T. J. and Yoon, J. K. (2007a). Dynamic expression of R-spondin family genes in mouse development. *Gene Expr. Patterns* **3**, 306-312.
Nam, J. S., Park, E., Turcotte, T. J., Palencia, S., Zhan, X., Lee, J., Yun, K., Funk, W. D. and Yoon, J. K. (2007b). Mouse R-spondin2 is required for apical ectodermal ridge maintenance in the hindlimb. *Dev. Biol.* **311**, 124-135.
Parma, P., Radi, O., Vidal, V., Chaboissier, M. C., Dellambra, E., Valentini, S., Guerra, L., Schedl, A. and Camerino, G. (2006). R-spondin1 is essential in sex determination, skin differentiation and malignancy. *Nat. Genet.* **38**, 1304-1309.
Pinson, K. I., Brennan, J., Monkley, S., Avery, B. J. and Skarnes, W. C. (2000). An LDL-receptor-related protein mediates Wnt signalling in mice. *Nature* **407**, 535-538.
Regnier, C. H., Masson, R., Kedinger, V., Textoris, J., Stoll, I., Chenard, M.-P., Dierich, A., Tomasetto, C. and TRio, M.-C. (2002). Impaired neural tube closure, axial skeleton malformations, and tracheal ring disruption in TRAF4-deficient mice. *Proc. Natl. Acad. Sci. USA* **99**, 5585-5590.
Shiels, H., Li, X., Schumacker, P. T., Maltepe, E., Padrid, P. A., Sperling, A., Thompson, C. B. and Lindsten, T. (2000). Traf4 deficiency leads to tracheal malformation with resulting alterations in air flow to the lungs. *Am. J. Pathol.* **157**, 679-688.
Shu, W., Jiang, Y. Q., Lu, M. M. and Morrisey, E. E. (2002). Wnt7b regulates mesenchymal proliferation and vascular development in the lung. *Development* **129**, 4831-4842.
Sun, X., Mariani, F. V. and Martin, G. R. (2002). Functions of FGF signaling from the apical ectodermal ridge in limb development. *Nature* **418**, 502-508.
Tebar, M., Destree, O., deVree, W. J. A. and Ten Have-Opbrock, A. A. W. (2001). Expression of Tcf/Lef and sFrp and localization of β-catenin in the developing mouse lung. *Mech. Dev.* **109**, 437-440.
Tzarfaty-Majar, V., López-Alemany, R., Feinstein, Y., Gombau, L., Goldshmidt, O., Soriano, E., Muñoz-Cánoves, P. and Klar, A. (2001). Plasmin-mediated release of the guidance molecule F-spondin from the extracellular matrix. *J. Biol. Chem.* **276**, 28233-28241.
van Tuyl, M., Liu, J., Groenman, F., Ridsdale, R., Han, R. N. N., Venkatesh, V., Tibboel, D. and Post, M. (2006). Iroquois genes influence proximo-distal morphogenesis during rat lung development. *Am. J. Physiol. Lung Cell Mol. Physiol.* **290**, L777-L789.
Wang, Z., Shu, W., Lu, M. M. and Morrisey, E. E. (2005). Wnt 7b activates canonical signaling in epithelial and vascular smooth muscle cells through interactions with Fzd1, Fzd10, and Lrp5. *Mol. Cell. Biol.* **25**, 5022-5030.
Wei, Q., Yokota, C., Semenov, M. V., Doble, B., Woodgett, J. and He, X. (2007). R-spondin 1 is a high affinity ligand for LRP6 and induces LRP6 phosphorylation and β-catenin signaling. *J. Biol. Chem.* **282**, 15903-15911.
Weidenfeld, J., Shu, W., Zhang, L., Millar, S. E. and Morrisey, E. E. (2002). The Wnt7b promoter is regulated by TTF-1, GATA6, and Foxa2 in lung epithelium. *J. Biol. Chem.* **277**, 21061-21070.

Table S1. Limb malformations observed in E18.5 fetuses

Forelimb

	Number of fetuses exhibiting malformations (%)									
	Autopod		Radius		Ulna		Humerus		Scapula	
Genotype of fetus (number)	Left	Right	Left	Right	Left	Right	Left	Right	Left	Right
Rspo2$^{Tg/Tg}$;*Lrp6*$^{+/+}$ (39)	3 (8)	15 (38)	0	8 (20)	0	0	0	0	0	0
Rspo2$^{Tg/Tg}$;*Lrp6*$^{+/-}$ (32)	32 (100)	32 (100)	23 (72)	30 (94)	1 (3)	3 (9)	4 (12)	10 (32)	0	0
Rspo2$^{+/Tg}$;*Lrp6*$^{+/-}$ (58)	5 (8)	11 (19)	0	0	0	1 (2)	0	0	0	0
Rspo2$^{+/+}$;*Lrp6*$^{+/-}$ (34)	0	0	0	0	0	0	0	0	0	0
Rspo2$^{+/+}$;*Lrp6*$^{+/+}$ (22)	0	0	0	0	0	0	0	0	0	0
Rspo2$^{+/Tg}$;*Lrp6*$^{+/+}$ (64)	0	0	0	0	0	0	0	0	0	0
Rspo2$^{+/+}$;*Lrp6*$^{-/-}$ (21)	21 (100)	21 (100)	7 (33)	6 (28)	1 (5)	2 (9)	0	0	0	0
Rspo2$^{+/Tg}$;*Lrp6*$^{-/-}$ (11)	11 (100)	11 (100)	6 (54)	6 (54)	7 (64)	7 (64)	2 (18)	3 (27)	0	0
Rspo2$^{Tg/Tg}$;*Lrp6*$^{-/-}$ (3)	3 (100)	3 (100)	3 (100)	3 (100)	3 (100)	3 (100)	3 (100)	3 (100)	3 (100)	2 (66)

Hindlimb

	Number of fetuses exhibiting malformations (%)							
	Autopod		Tibia		Fibula		Femur	
	Left	Right	Left	Right	Left	Right	Left	Right
Rspo2$^{Tg/Tg}$;*Lrp6*$^{+/+}$ (39)	36 (92)	32 (82)	0	1 (2)	32 (82)	21 (54)	0	0
Rspo2$^{Tg/Tg}$;*Lrp6*$^{+/-}$ (32)	32 (100)	32 (100)	31 (97)	30 (94)	32 (100)	32 (100)	27 (84)	23 (72)
Rspo2$^{+/Tg}$;*Lrp6*$^{+/-}$ (58)	2 (3)	1 (2)	0	1 (2)	0	0	0	0
Rspo2$^{+/+}$;*Lrp6*$^{+/-}$ (34)	0	0	0	0	0	0	0	0
Rspo2$^{+/+}$;*Lrp6*$^{+/+}$ (22)	0	0	0	0	0	0	0	0
Rspo2$^{+/Tg}$;*Lrp6*$^{+/+}$ (64)	0	0	0	0	0	0	0	0
Rspo2$^{+/+}$;*Lrp6*$^{-/-}$ (21)	21 (100)	21 (100)	11 (52)	11 (52)	21 (100)	21 (100)	5 (24)	5 (24)
Rspo2$^{+/Tg}$;*Lrp6*$^{-/-}$ (11)	11 (100)	11 (100)	11 (100)	11 (100)	11 (100)	10 (91)	9 (82)	6 (54)
Rspo2$^{Tg/Tg}$;*Lrp6*$^{-/-}$ (3)	3 (100)	3 (100)	3 (100)	3 (100)	3 (100)	3 (100)	3 (100)	3 (100)

Table S2. Laryngeal and tracheal malformations in E18.5 fetuses

Genotype	*n*	Number of fetuses with malformed cartilages (%)					
		Thyroid	Arytenoid fused to cricoid	Cricoid lamina open	Normal tracheal rings	Bifurcared tracheal rings	Cartilage nodules
Rspo2$^{+/+}$;*Lrp6*$^{+/+}$	11	0	0	0	11 (100%)	8 (73%)	2 (18%)
Rspo2$^{+/Tg}$;*Lrp6*$^{+/+}$	17	0	0	0	17 (100%)	15 (88%)	4 (23%)
Rspo2$^{+/Tg}$;*Lrp6*$^{+/-}$	13	0	0	0	13 (100%)	12 (92%)	3 (23%)
Rspo2$^{Tg/Tg}$;*Lrp6*$^{+/+}$	17	4 (23%)	15 (88%)	17 (100%)	12 (71%)	5 (29%)	17 (100%)
Rspo2$^{Tg/Tg}$;*Lrp6*$^{+/-}$	9	3 (33%)	9 (100%)	9 (100%)	5 (55%)	2 (22%)	9 (100%)
Rspo2$^{Tg/Tg}$;*Lrp6*$^{-/-}$	2	2 (100%)	n.d.	n.p.	0	0	0
Rspo2$^{+/Tg}$;*Lrp6*$^{-/-}$	8	0	0	0	8 (100%)	8 (100%)	3 (37%)
Rspo2$^{+/+}$;*Lrp6*$^{-/-}$	5	0	0	0	5 (100%)	4 (80%)	0

n, number of fetuses; n.d., not determinable; n.p., not present.

Table S3. Tracheal cartilage defects upon removal of epithelial β-catenin

Genotype	*n*	Number of fetuses with tracheal ring phenotype (%)				
		Normal rings	Bifurcated fused rings	Abnormally shaped or nodules		Ring half open ventrally
Doxycyline prior to E13.5				1 or 2	>2	
Tg(SftpC-rtTA)$^{-/-}$; Tg(Tet0$_7$CMV-cre)$^{+}$; β-catenin$^{+/flox}$	13	13 (100%)	10 (77%)	7 (54%)	0	1 (8%)
Tg(SftpC-rtTA)$^{-/-}$; Tg(Tet0$_7$CMV-cre)$^{+}$; β-catenin$^{flox/flox}$	8	8 (100%)	8 (100%)	4 (50%)	0	0
Tg(SftpC-rtTA)$^{+}$; Tg(Tet0$_7$CMV-cre)$^{+}$; β-catenin$^{+/flox}$	14	11 (78%)	4 (29%)	2 (14%)	2 (14%)	4 (29%)
Tg(SftpC-rtTA)$^{+}$; Tg(Tet0$_7$CMV-cre)$^{+}$; β-catenin$^{flox/flox}$	13	11 (85%)	9 (69%)	2 (15%)	6 (46%)	13 (100%)

n, number of fetuses examined.